Calmodulin-containing substructures of the centrosomal matrix released by microtubule perturbation

Nicoleta Moisoi, Muriel Erent*, Sheena Whyte, Stephen Martin and Peter M. Bayley‡

Division of Physical Biochemistry, National Institute for Medical Research, Mill Hill, London NW7 1AA, UK

*Present address: Department of Biophysics, Max Planck Institute for Medical Research, Jahnstrasse 29, D-69120 Heidelberg, Germany

‡Author for correspondence (e-mail: pbayley@nimr.mrc.ac.uk)

Accepted 12 March 2002

Journal of Cell Science 115, 2367-2379 (2002) *© The Company of Biologists Ltd*

Summary

Calmodulin redistribution in MDCK and HeLa cells subjected to microtubule perturbations by antimitotic drugs was followed using a calmodulin-EGFP fusion protein that preserves the Ca^{2+} affinity, target binding and activation properties of native calmodulin. CaM-EGFP targeting to spindle structures in normal cell division and upon spindle microtubule disruption allows evaluation of the dynamic redistribution of calmodulin in cell division. Under progressive treatment of stably transfected mammalian cells with nocodazole or vinblastine, the centrosomal matrix at the mitotic poles subdivides into numerous small 'star-like' structures, with the calmodulin concentrated centrally, and partially distinct from the reduced microtubule mass to which kinetochores and chromosomes are attached. Prolonged vinblastine treatment causes the release of localised calmodulin into a uniform cytoplasmic distribution, and tubulin paracrystal formation. By contrast, paclitaxel treatment of metaphase cells apparently causes limited disassembly of the pericentriolar material into a number of multipolar 'ring-like' structures containing calmodulin, each one having multiple attached microtubules terminating in the partially disordered kinetochore/chromosome complex. Thus drugs with opposite effects in either destabilising or stabilising mitotic microtubules cause subdivision of the centrosomal matrix into two distinctive calmodulin-containing structures, namely small punctate 'stars' or larger polar 'rings' respectively. The 'star-like' structures may represent an integral subcomponent for the attachment of kinetochore microtubules to the metaphase centrosome complex. The results imply that microtubules have a role in stabilising the structure of the pericentriolar matrix, involving interaction, either direct or indirect, with one or more proteins that are targets for binding of calmodulin. Possible candidates include the pericentriolar matrix-associated coiled-coil proteins containing calmodulin-binding motifs, such as myosin V, kendrin (PCNT2) and AKAP450.

Movies available on-line

Key words: Calmodulin-EGFP, Antimitotic drugs, Calmodulin-targets

Introduction

Calmodulin (CaM), the prototypical example of the EF-hand family of Ca^{2+} sensing proteins, is expressed in all eukaryotic cells, where it participates in signalling pathways that regulate many crucial processes such as growth, cell-division, proliferation and movement (Chin and Means, 2000). The association of CaM with cytoskeletal elements during mitosis has been studied by immunofluorescence, immuno-electron microscopy (Welsh et al., 1979; De Mey et al., 1980; Willingham et al., 1983) and micro-injected fluorescently-labeled CaM (Zavortink et al., 1983; Stemple et al., 1988). CaM was deduced to be present in metaphase at kinetochore-to-pole microtubules, in anaphase in the two half spindles, appearing in late anaphase in the interzone region and in telophase at distal regions of the midbody. The presence of CaM near kinetochores in normal, nocodazole- and colcemid-treated cells was previously reported, but not characterised in detail (Sweet et al., 1988; Mitsuyama and Kanno, 1993). Recently, the CaM-EGFP fusion protein was used to follow the structural localisation of CaM in subcellular domains and its distribution in different stages of the cell cycle (Erent et al., 1999; Li et al., 1999). While calmodulin and microtubules are closely associated in dividing cells, there appears to be no direct interaction between them in vivo.

Antimitotic drugs perturbing the cytoskeletal system (colchicine-nocodazole-podophyllotoxin, vinca alkaloids and taxoids) have been widely used to study cellular processes dependent on the microtubule network integrity. These affect microtubule polymerisation and dynamics by different molecular mechanisms and with different sensitivities. The first two classes are highly effective as microtubule depolymerising agents, in vitro and in vivo. In the latter case this can lead to dispersal of the pericentriolar material (PCM), which surrounds centrioles in the centrosome. However, at low concentration, the same drugs inhibit the dynamic instability of microtubules and can stabilise the spindle in vivo (Wadsworth and McGrail, 1990; Jordan et al., 1992; Martin et

al., 1993; Sellitto and Kuriyama, 1988; Jordan and Wilson, 1998; Jordan and Wilson, 1999; Ngan et al., 2001).

Four stages of the time- and concentration-dependent disruption of microtubule distribution in the mitotic spindle have been distinguished by treatment of mitotic cells with nocodazole and vinca-alcaloids (Jordan et al., 1992). Stage I is characterised by the arrest of spindle growth and dynamics due to inhibition of microtubule dynamic instability. Stage II shows a shortening of spindle due to loss of labile microtubules. Stage III is defined by the appearance of 'star-like' structures in mono- or poly-aster shape with some apparently drug- (or cold-) resistant microtubule structures, and stage IV, showing full disassembly and loss of organisation of the mitotic spindle, is characterised by punctate distribution of tubulin and few residual microtubules.

The third class of drugs, the taxoids, act as microtubule-stabilising agents, favouring microtubule polymerisation. At high concentration, microtubule mass increases and bundling occurs with severe spatial disruption, and the creation of multiple spindles compromises the organising capacity of centrosomes and kinetochores (De Brabander et al., 1981). At low concentration, the spindle is stabilised since its microtubule dynamics are suppressed (Jordan and Wilson, 1998; Jordan and Wilson, 1999). Pulsed treatment of synchronised interphase HeLa cells with taxoids causes aberrant mitotic structures and catastrophic exit from mitosis (Paoletti at al., 1997).

In the present work, we have stably transfected cells with CaM-EGFP, and used epifluorescence microscopy and deconvolution to follow the CaM redistribution in fixed or in live cells. This approach allows quantification of the continuous redistribution of the fusion protein in a given cell and, by further mutation of CaM-EGFP, one can study the calcium sensitivity of calmodulin-cytoskeletal interactions. To validate the approach, we established that CaM-EGFP fusion protein preserves the properties of wtCaM, and that the expression of CaM-EGFP does not interfere with normal mitotic behaviour of the cell. We have then used typical antimitotic drugs, namely nocodazole, vinblastine, paclitaxel (taxol^{TM}) to study the distribution of CaM-EGFP in different stages of mitotic spindle impairment, comparing their actions with mitotic spindle disruption by cold treatment.

We show that classes of drugs that act in opposite directions, either polymerising or depolymerising microtubules, both release distinctive subclasses of CaM-target complexes from mitotic structures. A major part of this CaM redistribution in the mitotic spindle derives from the pericentriolar matrix. Under microtubule perturbation this divides into calmodulin-containing subcomponents, seen distinctively either as small 'star-like' structures in treatment with microtubule disruptive drugs, or as multipolar 'ring-like' structures in treatment with paclitaxel.

Materials and Methods

Plasmids

pN3-XeCaM-EGFP: wild-type *Xenopus* calmodulin fusion protein with EGFP (CaM-EGFP) mammalian expression vector was prepared as previously described (Erent et al., 1999). pET24d-XeCaM-EGFP: the coding region for XeCaM-EGFP was excised from a pTRE vector previously prepared (Erent et al., 1999) using a partial *Nco*I-*Not*I digest. A modified pET24d (cf. Gregorio et al., 1998) vector was digested with *Nco*I-*Not*I, and the XeCaM-EGFP coding region was inserted by ligation. This allowed inducible expression of XeCaM-EGFP (CaM-EGFP) from bacterial cells with GST and hexa-His tags for ease of purification.

Protein expression and purification

Bacterial cell cultures, *E. coli* BL21 DE3 (Stratagene), transformed with pET24d-XeCaM-EGFP were induced with 1 mM IPTG for 4 hours. The cultures were centrifuged and the pellet resuspended in PBS and lysed by sonication for 5 minutes, 4°C, at half power on 50% cycle with a Vibra Cell Sonicator (Sonics and Materials, Danbury, CT). After centrifugation the 6His-GST-CaM-EGFP fusion protein contained in the supernatant was further purified using a GST column following the manufacturer's instructions (Pharmacia-Biotech). The protein was dialysed overnight at 4°C and concentrated using the Amincon Diaflow system with a 10 kDa cut-off membrane. The 6His-GST fragment was cleaved using Tobacco Etch Virus protease (Gibco-BRL). Separation of CaM-EGFP and 6His-GST was obtained by further purification on Ni-NTA column. CaM-EGFP was present in the flow through. The protein was concentrated and desalted on PD10 for in vitro experiments. Purity was tested on SDS-PAGE and Western blot. The final concentration of CaM-EGFP was 31.8 μM.

Spectroscopic measurements

Calcium binding to CaM-EGFP was studied using the chromophoric calcium chelator 5,5′-Br_2BAPTA as described (Linse et al., 1988; Linse et al., 1991; Martin et al., 1996). Absorption measurements were made on a Cary 3E spectrophotometer at 20°C, using typically 23 μM CaM-EGFP and 28 μM 5,5′-Br_2BAPTA at 20°C in 10 mM Tris, 100 mM KCl, pH 8. 'Ca^{2+}-free buffer' was made by Chelex treatment and the residual Ca^{2+} concentration was less than 0.6 μM.

Fluorescence measurements

The binding of peptide WFF (NH2-KKRWKKNFIAVSAANRFK-CO_2H, residue 1-18 of the M13 target sequence of skeletal muscle myosin light chain kinase, skMLCK) to CaM-EGFP was studied by following changes in fluorescence upon addition of peptide to CaM-EGFP (in 0.5 μM). The fluorescence was recorded using a SPEX FluoroMax fluorimeter at 20°C in UV-transmitting plastic cuvettes. The buffer comprised 25 mM Tris and 100 mM KCl, pH 8.

Cell culture (MDCK and HeLa Tet-On cells)

Transient or stably transfected cells were obtained by a liposome-mediated method (MDCK) or by electroporation (HeLa Tet-On). For stable cell lines the cells were co-transfected with pN3-XeCaM-EGFP (constitutive expression under the control of the CMV promoter) and pTK-Hyg (Clontech) for hygromycin resistance and selected with 0.3 mg/ml hygromycin. Cells were grown in DMEM (Gibco BRL, cat No. 41966-029), 10% FCS, 0.1 mg/ml G418 (neomycin), 0.05 mg/ml gentamycin, (0.1 mg/ml hygromycin in the stable cell lines). We used the following stable cell lines: HeLa Tet-on for constitutive expression of XeCaM-EGFP, clone A5; MDCK with constitutive expression of XeCaM-EGFP, clone 8; and MDCK and HeLa Tet-on transiently transfected with the plasmid pN3-EGFP (Clontech) for control experiments. The morphology of the CaM-EGFP at a given stage of mitotic spindle disruption, was essentially similar in HeLa and MDCK, although the latter divide more rapidly. As a control, the distribution of CaM-EGFP was recorded for each type of treatment in fixed cells without staining for cytoskeletal elements. CaM-EGFP was expressed at <5% endogenous CaM level, which was determined in antiCaM antibody Western blots of cell lysates (cf. Erent et al., 1999).

Immunofluorescence studies

Cells were grown on coverslips and either fixed in 3% paraformaldehyde (PFA, Sigma) at room temperature, or fixed and extracted before immunostaining. For microtubule and kinetochore immunostaining, fixation and extraction was in microtubule stabilising buffer (100 mM PIPES, pH 7.0, 1 mM $MgCl_2$, 5 mM EGTA), containing 0.5 μM Taxol™, 4% (w/v) polyethylene glycol, 3% PFA and 0.2% Triton X-100. Microtubule immunostaining was performed with anti-α-tubulin antibody (Serotec) (1:100 in 1% BSA/PBS) and with (1:100) either anti-rat Cy-3-, Cy-5- or TRITC-conjugated secondary antibody (Sigma, Dako). Kinetochores were labeled using human CREST serum at 1:2500 dilution. Secondary antibody, TRITC-conjugated goat anti-human IgG (H+L) (Jackson-ImmunoResearch) was used at 1/100 dilution. For double staining of kinetochores and microtubules, kinetochore labeling was followed by extensive washing with PBS prior to microtubule staining with Cy-5-labeled secondary antibody. In all cases the cells were co-stained for DNA with Hoechst 33342, (Molecular Probes; 1:1000 in distilled water from 10 mg/ml stock), for 2 minutes at room temperature, then mounted with Mowiol (CalBiochem) after washing four times in PBS.

Epifluorescence microscopy was performed on living or fixed cells, using an Olympus IX70 inverted microscope and an Olympus U-Plan-Apo 100× objective (NA 1.35). Images were recorded on a cooled CCD camera (Photometrics CH350L; Sensor, Kodak KAF1400; 1317×1035 pixels). Typically 20-25 optical sections were taken, through focus z step 0.2 μm; the images were deconvolved (~15 iterations) and quantitatively analysed using Deltavision software (Applied Precision, Seattle) on a Silicon Graphics workstation, and the final images (usually projected series) were further processed in Adobe PhotoShop. The experiments were normally repeated two or three times and the images presented are representative of at least 20 similar images.

Antimitotic treatments

Nocodazole was applied (1-6 hours) in culture medium at concentrations 0.01-10.00 μg/ml. Recovery was followed for 4 hours after the 6 hour treatment with 0.1 μg/ml. Vinblastine was applied from 0.5-100.0 nM (1 hour) and 1 μM (4 hours). Cold treatment of cells (4°C) was for 0.25-2.00 hours. Paclitaxel (10 nM and 10 μM) was applied for 4 hours.

Results

Characterisation of CaM-EGFP properties in vitro and in vivo

The absorption properties of the purified fusion protein were studied under different levels of Ca^{2+} saturation. Fig. 1A (and inset) shows that there is little or no effect on the absorption of CaM-EGFP at 489 nm, over the physiological range of [Ca^{2+}] (0-10 μM); higher concentrations show a systematic small change attributable to nonspecific effects. At 280 nm there is a marked change in the absorbance of the single Tyr residue, as observed for wtCaM; Fig. 1B shows that CaM-EGFP competes with Br_2BAPTA (similarly to wtCaM), consistent with the average Ca^{2+} affinity of the calmodulin (~5 μM) (Browne et al., 1997) being unaffected by the EGFP moiety. Western blotting (data not shown) with anti-CaM antibody (Sacks et al., 1991),

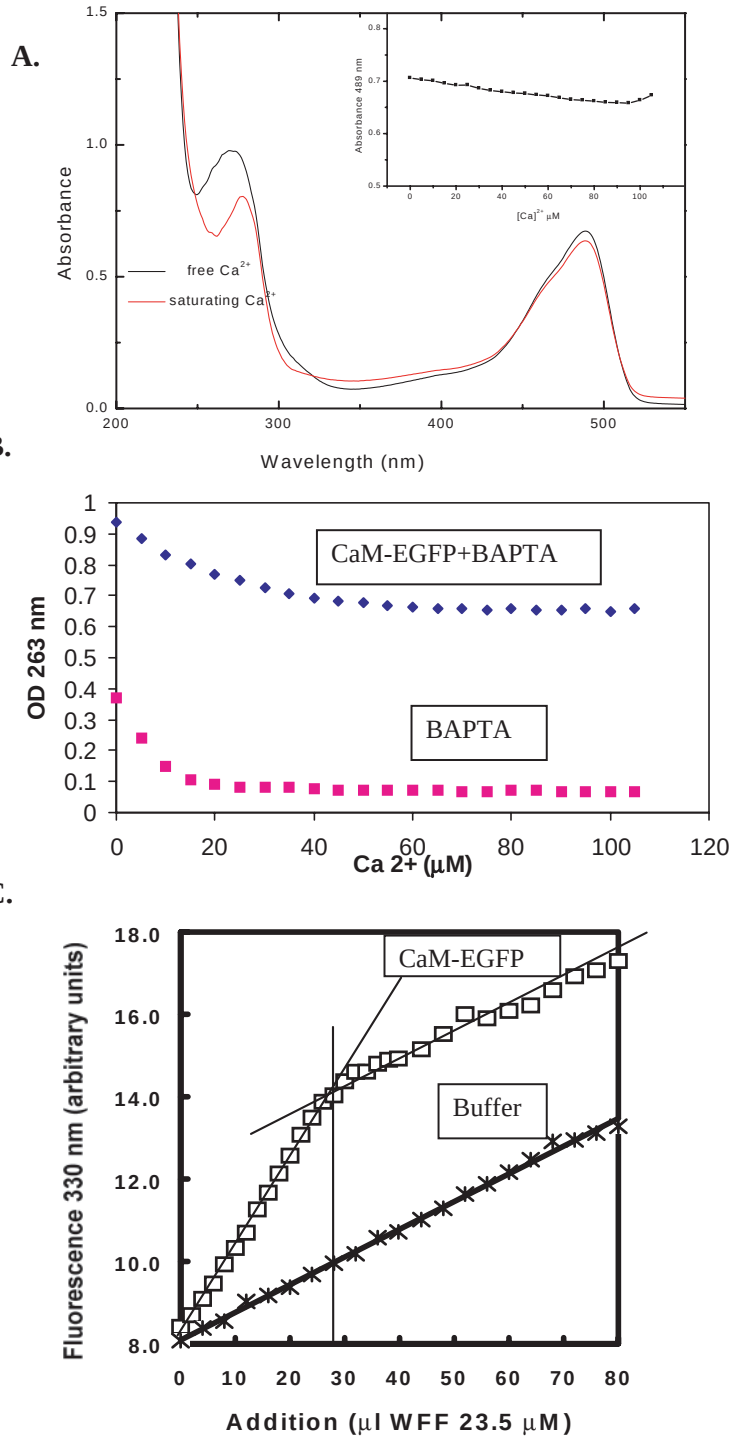

Fig. 1. Spectroscopic properties of CaM-EGFP prove that the fusion protein preserves the CaM characteristics with respect to calcium and peptide binding. (A) Absorption spectra of CaM-EGFP: Ca^{2+}-free and with saturating Ca^{2+}; inset: CaM-EGFP absorbance (489 nm) with Ca^{2+} titration. Different Ca^{2+} saturation levels do not affect the EGFP characteristic absorption spectra (with maximum at 489 nm); at 280 nm there is the same change in the single Tyr absorbance as for wtCaM. (B) Ca^{2+} titration of CaM-EGFP: 5,5′-Br_2BAPTA absorbance at 263 nm; CaM-EGFP competes with Br_2BAPTA showing no change of the average Ca^{2+} affinity of the fusion protein compared with wtCaM. (C) WFF peptide fluorescence titration of Ca^{2+}-saturated CaM-EGFP (λ_{ex}=290 nm, λ_{em}=330 nm) indicates a 1:1 stoichiometry and dissociation constant similar to that of wtCaM.

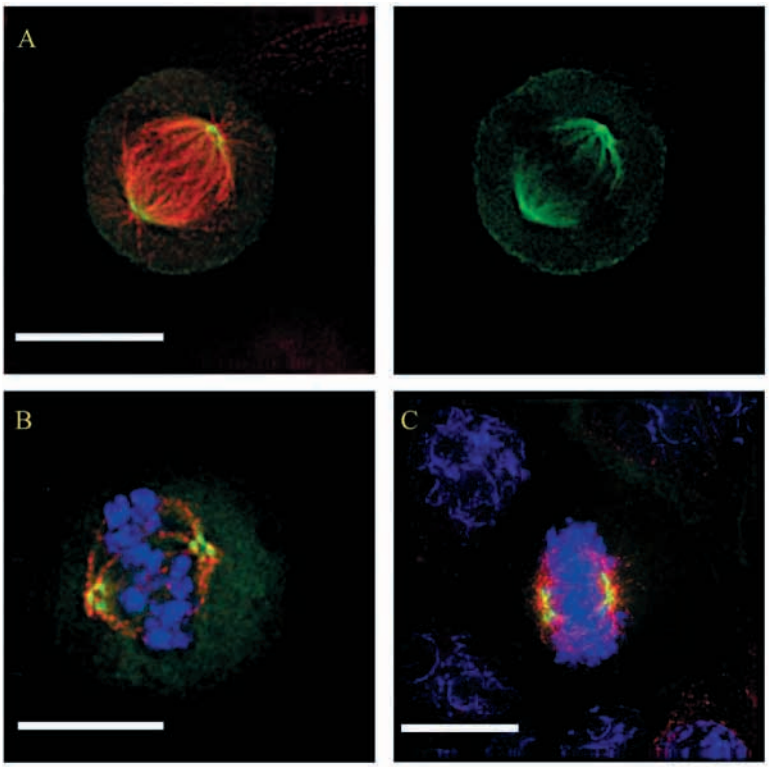

Fig. 2. Calmodulin distribution in the mitotic spindle in control cells and in mild treatment with nocodazole. (A) Control metaphase HeLa (projection of deconvolved sections). (B) Stage I: MDCK (nocodazole 0.01 μg/ml, 2 hours; one section deconvolved). (C) Stage II: MDCK (nocodazole 0.01 μg/ml, 2 hours; projection of deconvolved section; adjacent panel shows only the CaM-EGFP (green) of the same cell). In the control, as in the first two stages of the mitotic spindle perturbation with depolymerising drug, CaM-EGFP is located at polar level in a ring-like pattern, and in the mitotic spindle along microtubules from pole to kinetochore with a decreasing intensity (green, CaM-EGFP; red, α-tubulin; blue, chromosomes). Bar, 10 μm.

shows the expected gel shift in the presence of Ca^{2+}, for both the purified CaM-EGFP and the expressed CaM-EGFP present in cytoplasmic lysates of MDCK-clone 8 and HeLa-clone A5.

Fig. 1C shows a typical in vitro target interaction of CaM-EGFP; the titration of CaM-EGFP with peptide WFF (see Materials and Methods) is monitored by the fluorescence change of the single Trp residue in the peptide (Findlay et al., 1995). The end point indicates a 1:1 stoichiometry, and a dissociation constant K_d<<0.2 nM [compare wtCaM, K_d ~0.01 nM (Browne et al., 1997)]. In addition, the fusion protein gave >95% Ca^{2+}-dependent activation of a truncation mutant 1-321 of calmodulin kinase I (Yokokura et al., 1995), with a K_{CaM} of 5±1 nM (compare CaM 100%, K_{CaM}=3.8±0.6 nM). These results confirm that the fusion protein of CaM-EGFP preserves the typical peptide-binding properties of CaM, and fully activates a typical CaM-dependent kinase.

GFP-based fluorophores are sensitive to pH changes (Lopis et al., 1998; Kneen et al., 1999). Our construct shows a (95% reversible) decrease in fluorescence (in fixed and living cells) for short exposures to pH 5-7, due to protonation of the chromophore. Longer exposures of the fluorophore to low pH induce irreversible denaturation and loss of fluorescence. Thus the fusion protein would be suitable for qualitative and quantitative studies of transient pH changes at CaM-targets in living cells.

Localisation of CaM-EGFP under conditions of microtubule perturbation

Microtubule disruption by nocodazole

The effect of mild nocodazole treatment on CaM-EGFP distribution in relation to the level of changes in the mitotic spindle is shown in Fig. 2. In untreated HeLa cells (Fig. 2A; see Fig. 4A for a MDCK control), CaM is distributed at the spindle poles in a dense structure around centrosomes and along the pole to kinetochore microtubules without accumulation at the kinetochores. The centrosomal matrix is a complex 3D structure that appears ring-like in projection (Moudjou et al., 1996; Dictenberg et al., 1998; Erent et al., 1999). Fig. 2B shows stage I of microtubule disruption in MDCK cells; the bipolar spindle is normal except for the small displacement of a few chromosomes from the metaphase plate. In Fig. 2C (stage II), the bipolar spindle is significantly shorter, and the microtubules and chromosomes exhibit more extensive rearrangements. In these two stages of microtubule disruption (as in controls), CaM-EGFP is concentrated at the ring-like polar centrosome, with decreasing gradient along spindle microtubules.

With increased nocodazole concentration, (Fig. 3, stage III), characteristic small sub-structures are observed, with calmodulin concentrated centrally and containing short residual kinetochore microtubules. Small star-like microtubule structures were observed on drug-treatment of HeLa cells (Jordan et al., 1992), and we retain this terminology. There is partial overlap between CaM-EGFP and tubulin staining, as observed for the centrosomal matrix (Erent et al., 1999) (Fig. 2A). Fig. 3i and ii show that multiple CaM-containing ‘stars’ can coexist with a remnant of the centrosomal structure, which largely lacks attached kinetochore microtubules and chromosomes. Thus microtubule disassembly has resulted in the separation from the matrix of multiple copies of a substructure involved in the attachment of kinetochore microtubules, linking the PCM to kinetochores and chromosomes. This star-like polar microtubule-CaM substructure is progressively lost with more extended drug

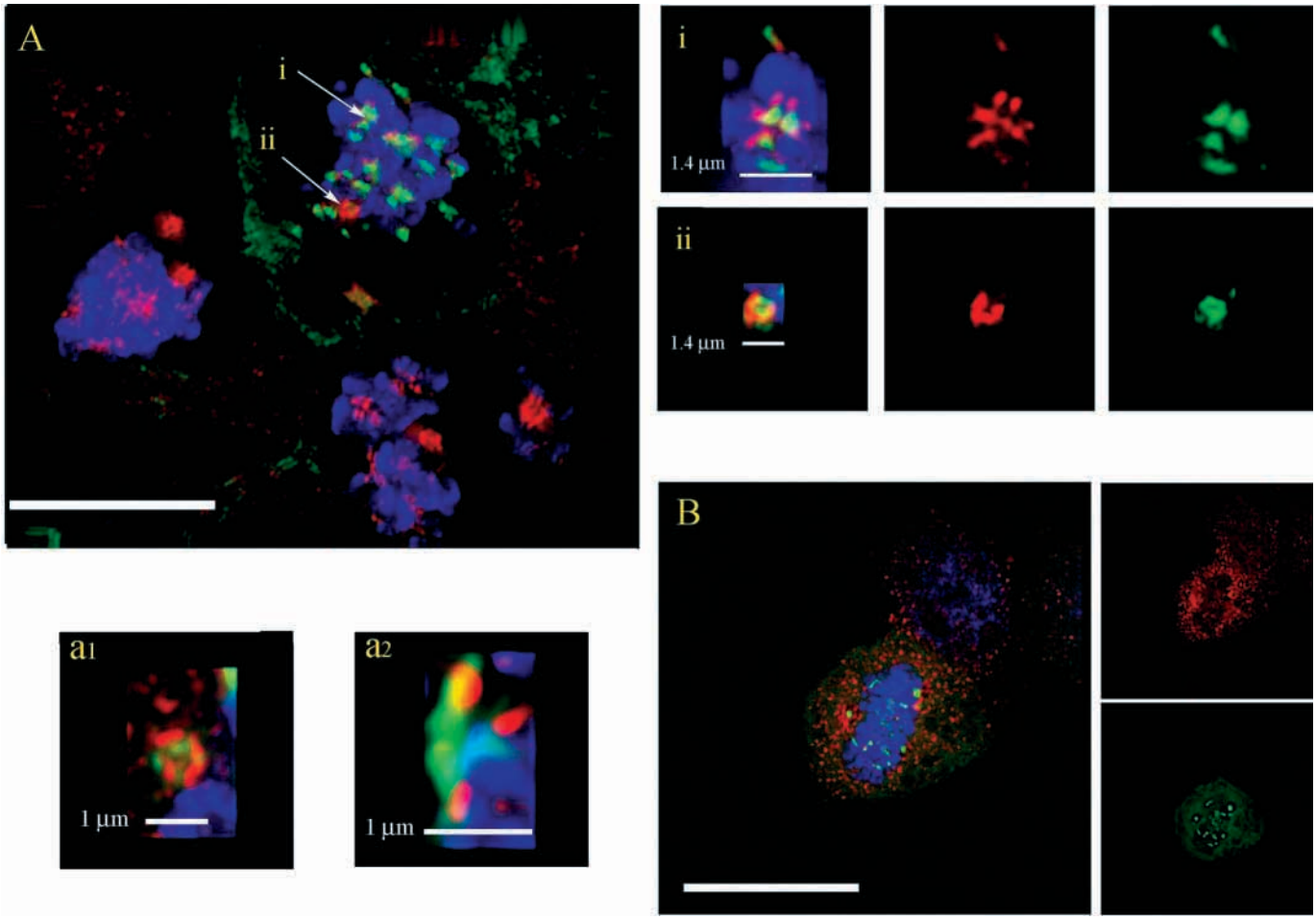

Fig. 3. Effect of nocodazole (6 hours, 0.1 μg/ml) on CaM-EGFP localisation in MDCK cells. (A) Stage III of microtubule disruption; (i) star-like structure; (ii) centrosomal remnant; (a_1) centrosomal remnant; (a_2) star-like structure in control experiments with cold treatment (4°C, 15 minutes to 2 hours). The star-like substructure shows the CaM-EGFP concentrated centrally with short microtubules radiating from it and the chromosomal material present at the outermost region. The centrosomal remnants show an alternating pattern of tubulin and CaM-EGFP with no obvious colocalisation, seen as 'ring' in projection. (B) Stage IV shows CaM location at kinetochore level in the absence of residual microtubules as seen with immunofluorescence. No centrosomal remnants could be seen (green, CaM-EGFP; red, α-tubulin; blue, chromosomes; projection of deconvolved series). Bar, 10 μm.

treatment. At stage IV of microtubule disruption (Fig. 3B) CaM localises in punctate densities, often paired and presumably in proximity to kinetochores, with little residual microtubule material being evident. Stage IV is the maximum level of perturbation induced with nocodazole in both HeLa and MDCK, and up to this stage, the nocodazole arrest is reversible.

In the same stages of microtubule disruption by nocodazole, staining of kinetochores with CREST serum shows the localisation of CaM close to kinetochores. In untreated cells (Fig. 4A), the CaM is located at the spindle poles and distributed along microtubules, but is less visible due to the strong staining at the poles. The kinetochores show their normal paired distribution aligned at the metaphase plate. After nocodazole treatment to stage IV (Fig. 4B,C), CaM shows similar distribution to microtubules localising close to kinetochores. The magnified images (Fig. 4B,C) show CaM concentrated centrally, with radiating microtubules linked to kinetochores and chromosomes at the outermost part.

Several controls were performed for these experiments. GFP alone did not localise to the star-like structures observed after nocodazole treatment of cells transiently transfected with *pN3-EGFP* plasmid (Clontech). To address the question whether the redistribution of CaM under the action of microtubule-disrupting drugs and the appearance of the star-like structure and the other types of CaM-microtubule association are due to nocodazole itself, a completely independent microtubule disruption method was used, namely, extended cold treatment at 4°C. This produces patterns of cytoskeletal distribution of the CaM-EGFP that are closely similar to the microtubule disruption induced by drugs. CaM and microtubules are found in the same star-like structure (Fig. 3a_2) as those observed in drug treatment. Thus CaM also localises close to the kinetochore in cold-treated cells, suggesting the absence of residual microtubules, and implying that kinetochore microtubules have shortened but not disappeared. There are also present spindle pole remnants (Fig. 3a_1) with alternating distribution of CaM-EGFP and microtubules. The

chromosomal material retains its organisation at the metaphase plate to a greater degree than is found with drug treatment.

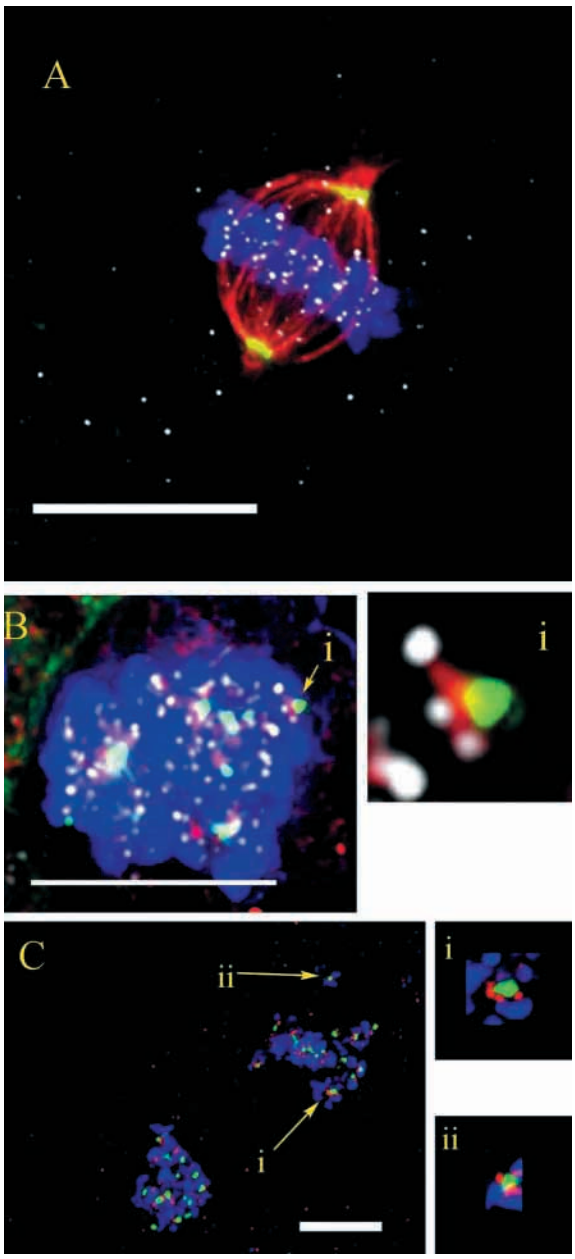

Fig. 4. CaM-EGFP redistribution in relation to kinetochores and microtubules in MDCK. (A) Metaphase MDCK control (no drug). (B) Star-like structures in nocodazole (0.1 μg/ml, 4 hours)-treated MDCK. The control cell shows the calmodulin (green) concentrated at the spindle pole in a ring-like shape, the microtubules (red; overlapping green and red seen as yellow) and the kinetochores (white, false colour) at the metaphase plate (blue). The star-like structure in stage III of mitotic spindle disruption seen with four colours gives the detailed arrangement of the four elements (B, detail shown in inset i): calmodulin as a core with radiating microtubules and the corresponding kinetochores attached to chromosomes. (C) CaM-EGFP redistribution relative to kinetochores induced with nocodazole in stage IV of spindle disruption. The kinetochores (red) are situated in immediate proximity to the CaM-EGFP (green) accumulation and chromosomes (blue). Bar, 10 μm.

Microtubule disruption by vinblastine

Vinblastine treatment shows significant effects on microtubules at lower extracellular concentrations and shorter incubation times compared with nocodazole. At low concentration it suppresses dynamic processes without changing the overall microtubule polymer mass; at intermediate concentrations microtubule assembly is inhibited and microtubules depolymerise; at higher concentrations microtubules are fully disassembled, and the drug can induce the aggregation of tubulin into paracrystals.

For stages I-III of the microtubule redistribution (Fig. 5A-D) the types of disposition of CaM relative to microtubules are the same as those with nocodazole. Further disruption shows little residual microtubule structure, with punctate tubulin and sometimes aggregates of tubulin. Two types of CaM distribution are observed: (1) a strong accumulation at the kinetochore level as seen for nocodazole treatment, also assigned to stage IV (Fig. 5E); and (2) when microtubules are fully depolymerised, a complete redistribution of the CaM throughout the cell (stage V; Fig. 5F). The final step, stage VI, denotes the appearance of tubulin paracrystals, which are formed in interphase as well as in dividing cells (Fig. 5G,H). The CaM was equally distributed throughout the cytoplasm, as in stage V.

In the vinblastine-treated cells, kinetochores are located at the periphery of the CaM-EGFP core, with progressive reduction of kinetochore microtubule length, (Fig. 5I-L). At prophase a radial pattern of CaM is observed with long filaments in the monopolar structure (Fig. 5I). At metaphase, multiple star-like structures are seen, (Fig. 5J, stage III), following microtubule shortening, eventually bringing the kinetochores very close to the CaM (Fig. 5K, stage IV). At stage V, the green CaM-EGFP, formerly co-localised close to kinetochores is now released throughout the cytoplasm. The punctate staining of kinetochores at stages V and VI (Fig. 5K,L) suggests that no major impairment has taken place in the kinetochore structure, implying that the CaM release correlates closely with the complete disassembly of the residual microtubules present in the star-like structures.

Images of live cells under vinblastine treatment (100 nM, ~1 hour) are shown in the supplementary material (http://jcs.biologists.org/supplemental). Movie 1 shows the initial spindle shortening corresponding to stages I and II. Movie 2 presents the full redistribution of CaM from control towards stages IV-V. CaM-EGFP redistribution to the proximity of kinetochores induced by the microtubule depolymerization and shortening appears to take place mainly through the subdivision of the polar structure into multiple ‘stars’. Movie 3 shows a relatively rare occurrence of a truncated polar microtubule/CaM structure as seen in fixed cells (Fig. 3ii; Fig. $3a_1$), simultaneous with ‘stars’ at kinetochores.

Action of paclitaxel – a microtubule polymerising drug

The uptake of taxoids in cells usually reaches much higher levels than the external concentration and the cellular effect of taxoids is difficult to reverse. Thus conditions of application may be critical. We have applied low concentrations of paclitaxel (10 nM) to MDCK cells, typically for four hours,

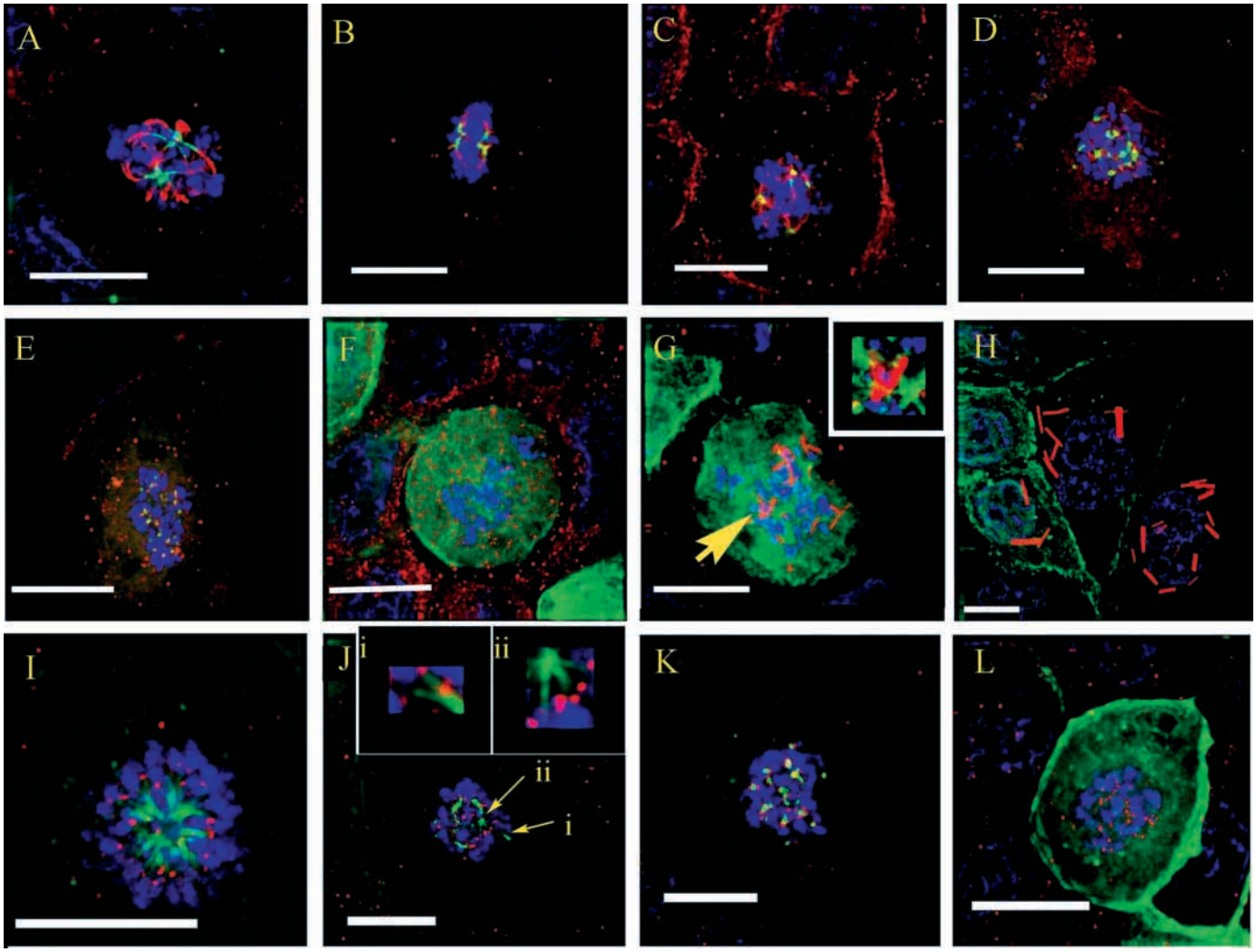

Fig. 5. CaM-EGFP redistribution in mitotic MDCKs under vinblastine treatment. Mitotic cells (A-G) stained for microtubules at different levels of spindle impairment (green, CaM-EGFP; red, α-tubulin; blue, chromosomes; projection of deconvolved sections). (A,B) (1 hour, 0.5 nM) Stages I and II with spindle shortening and CaM in a ring-like structure at spindle poles and along spindle microtubules with decreasing intensity. (C,D) (1 hour, 1 nM) Stage III with CaM at the cores of the star-like structures. (E) (1 hour, 10 nM) Stage IV shows the CaM in a punctate distribution but immunofluorescence does not identify remaining kinetochore microtubules. (F) (1 hour, 50 nM) Stage V with striking release of the calmodulin from the punctuate accumulation in an even cytoplasmic distribution. (G) (1 hour, 100 nM) Stage VI in which tubulin forms paracrystals, with a similar cytoplasmic distribution of CaM as in stage V. (H) (1 hour, 100 nM) Interphase cells with tubulin paracrystals. (I-L) Relative distribution of CaM-EGFP (green) and kinetochores (red) with chromosomes (blue) in vinblastine-treated MDCK cells (projection of deconvolved series). (I) (10 nM, 1 hour) At the arrest of mitosis in prophase in a monopolar spindle, the CaM shows the gradient distribution along microtubules. (J, stage III and K, stage IV) (0.5 nM, 1 hour) star-like structures (details shown in insets i and ii); the distance between the kinetochores and CaM core shortens progressively (K), and the CaM along the microtubule is progressively redistributed into the cytoplasm in the stage V (L; 100 nM, 1 hour). Bar, 10 μm.

conditions that did not induce the widespread occurrence of microtubule asters in interphase cells. By contrast, mitotic cells characteristically show well-developed monopolar, bipolar and some three and four polar structures (Fig. 6A-D). Few cells with more than four poles were observed in these conditions (Fig. 6E). Higher concentrations of taxol (10 μM) favour formation of multiple poles, although cells with three or four poles were also seen. These multipolar structures have extensive microtubule arrays that maintain the connection to the condensed chromosome plate. The multiple poles have a distinctive shape, which appears ring-like in projection, similar to the normal distribution of CaM in the spindle pole in untreated cells. Fig. 6A-E also shows the redistribution of CaM-EGFP relative to microtubules in mitotic cells. Surprisingly CaM-EGFP is located at all of the poles, although some of these will not contain centrioles (Vorobjev et al., 2000). The ring-like shape, as seen in projection at each of the poles, is strongly preserved. The monopolar spindle shows a single ‘ring’ of calmodulin at the minus ends of the microtubules, resulting from the accumulation of pericentriolar material of the two unseparated centrosomes. Although it is present along microtubules in the multiple spindles there is no evidence for the accumulation of CaM at the kinetochores themselves. The microtubule staining (Fig. 6B-D) and the

kinetochore labeling (Fig. 6F-I) show that the microtubule plus ends and the kinetochores remain aligned in the metaphase plate, which may appear segmented (Fig. 6D). The substructure formed by spindle microtubules and corresponding kinetochores and chromosomes generally retains its integrity but there is a major perturbation of CaM-

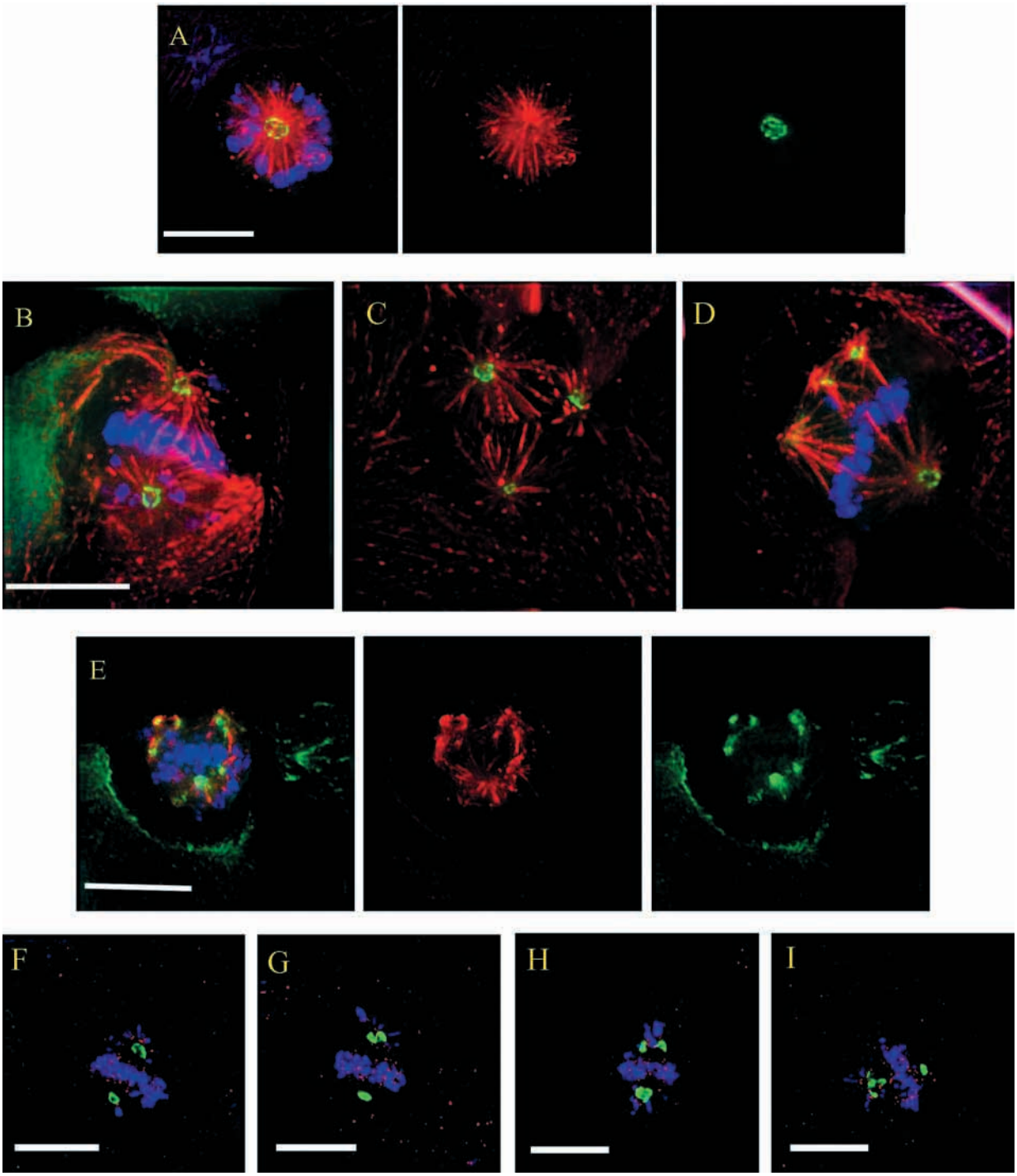

Fig. 6. (A-E) CaM-EGFP redistribution at the paclitaxel-induced microtubule polar structures in mitotic MDCKs (4 hours, 10 nM) (green, CaM-EGFP; red, α-tubulin; blue, chromosomes); (A) Monopolar spindle; (B) Bipolar spindle; (C) Three-polar spindle; (D) Quadri-polar spindle; (E) Multipolar spindle; Calmodulin redistributes in a ring-like shape at the paclitaxel-induced multipolar spindle without an accumulation at the kinetochores level. CaM-preserves the ring-like shape as seen in projection at every pole. Note that in the bipolar structure the CaM content at the two poles (B) is symmetrically distributed, and at the three (C) and four poles (D) its content decreases with the increasing number of poles. (F-I) Example of steps in the paclitaxel-induced multipolar structure as shown by CaM-EGFP at polar level (green, CaM-EGFP; red, kinetochore; blue, chromosomes). The CaM-containing ring-like structure divides (A,B), producing two or more poles (C,D). The kinetochores decorate chromosomes at the metaphase plate and those that were removed together with the related microtubules; projection of deconvolved series. Bar, 10 μm.

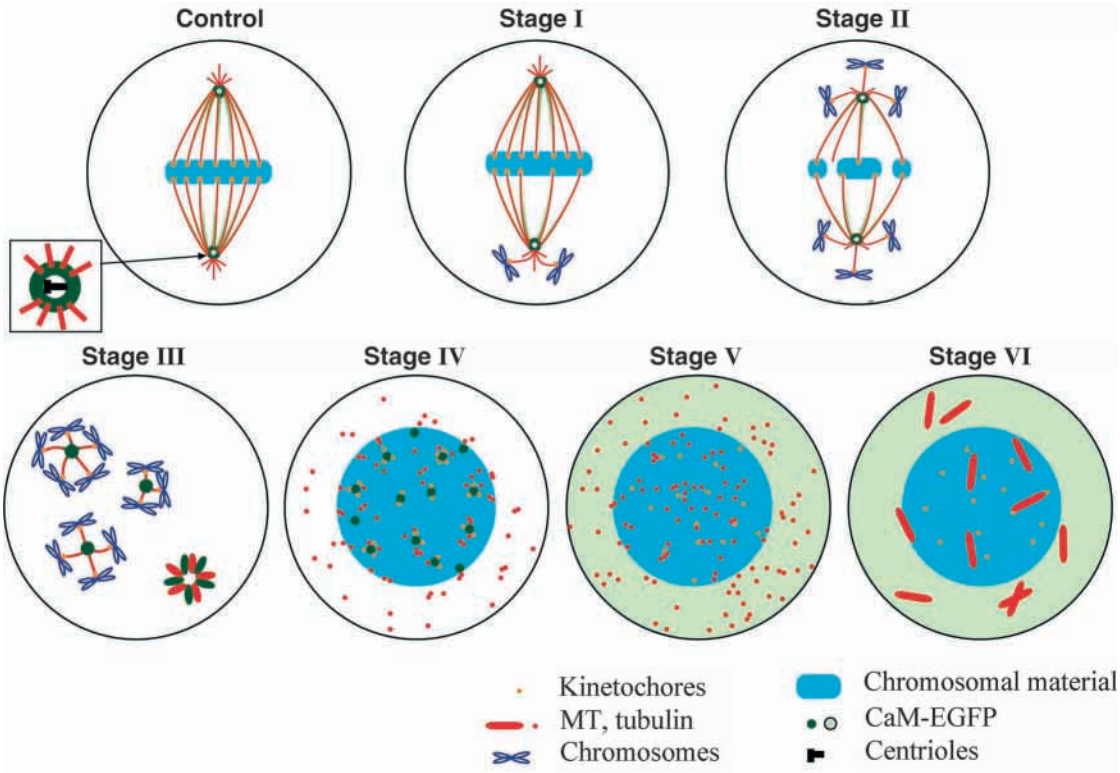

Fig. 7. Schematic view of steps in calmodulin redistribution under microtubule disrupting treatments. In control metaphase cells and in the stages I/II of microtubule spindle impairment, CaM preserves a ring-like structure at the spindle pole and the intensity distribution along microtubules decreases from poles to kinetochores. Stage III shows that the chromosomal matrix has divided, the kinetochores lose the metaphase alignment, tending to group around the CaM-containing cores and there is a punctate distribution of CaM, in multiple small star-like structures, associated via short residual microtubules to kinetochores/chromosomes together with the remnants of the calmodulin-microtubule polar structure. In stage IV, CaM-EGFP is close to kinetochores that are attached to the chromosome mass and tubulin is punctate. In stages V and VI (vinblastine only) there is a striking dispersion of the CaM from its accumulation sites in the cytosol and tubulin paracrystals are formed. Immunofluorescence and live cell monitoring suggest that the main mechanism of the CaM-EGFP redistribution throughout these stages is by the splitting of the pericentriolar material that contains the targets for calmodulin by shortening of the spindle microtubules until they are progressively removed.

EGFP at the spindle pole (Fig. 6F-I). This eventually leads to the subdivision of the centrosomal matrix into separate poles and associated spindle microtubules. Quantitative analysis of deconvolved images taken following a metaphase cell under paclitaxel perturbation (Movie 4) shows that 85-95% of the fluorescence intensity of CaM is conserved after the spliting of one normal spindle pole into two or three drug-induced CaM-containing polar structures. Therefore, the paclitaxel treatment appears to cause predominantly the splitting of the pre-existing centrosomal matrix. We show the splitting of a pre-existent centrosome in a dividing cell at metaphase under the effect of taxol (30 nM, ~20 minutes) in Movie 4.

Discussion

Effects on the pericentriolar matrix of drug-induced microtubule depolymerisation

The main difference in morphological changes to the spindle induced by the microtubule depolymerising drugs nocodazole, podophyllotoxin, vinblastine (Jordan et al., 1992; Jordan et al., 1999), vinflunine, vinorelbine (Ngan et al., 2001) is the level of impairment that each drug is able to induce over a range of concentrations and time of exposure, with vinca-alkaloids being generally 10-100-fold more effective. With increasing concentrations of depolymerising drugs, astral and pole-to-pole microtubules are first to be disrupted, followed by kinetochore-to-pole microtubules. The most resistant microtubule subclasses are the (anchored) kinetochore microtubules, which probably include microtubule-associated proteins. Nocodazole caused spindle disruption up to stage IV, when residual microtubules cannot be detected immunocytochemically but where CaM-EGFP remains punctate. Vinblastine produced two additional identifiable levels: stage V, with undetectable residual microtubules and total release of CaM-EGFP into the cytoplasmic space; and stage VI, coincident with tubulin paracrystal formation, showing the same uniform cytoplasmic distribution of calmodulin.

Using both immunostaining and in vivo imaging, the main source of CaM accumulated in the star-like structures at the kinetochores is from the polar ‘ring’, following the shortening of kinetochore-to-pole microtubules. The magnified images (see details in Fig. 3i,a_2; Fig. 4B,C) show that CaM is concentrated in the center of the star-like sub-structures, which

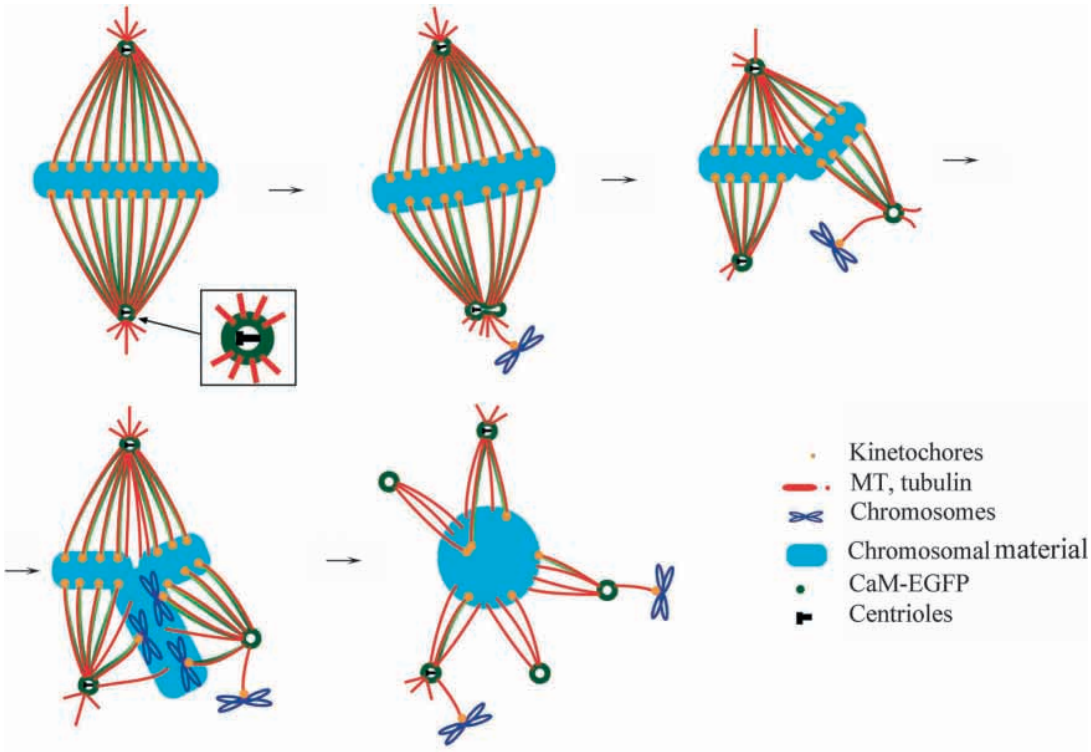

Fig. 8. Schematic view of steps in calmodulin redistribution under microtubule stabilising treatment with paclitaxel. The CaM initially remains associated with centrosomal matrix and kinetochore-to-pole microtubules, as in control cells. At the spindle pole the CaM-EGFP appears to subdivide from its ring-like shape, along with entire fragments of the spindle, including microtubules and associated kinetochores and chromosomes. Further repetition of this process generates a multipolar spindle, with CaM seen in a ring-like structure at each of these poles, some of which contain centrioles, and the chromosomal material becomes disorganised.

appears to identify a key element involved in maintaining the kinetochores around this core.

The steps in calmodulin redistribution following microtubule disruption are schematically depicted in Fig. 7. In control metaphase cells and the first two stages of microtubule spindle impairment, CaM preserves a ring-like structure at the spindle pole, and a continuous distribution along microtubules from poles to kinetochores. Stage III shows a star-like distribution of CaM, associated with residual microtubules. In stage IV there are no microtubules detected by immunofluorescence and calmodulin appears punctate, the kinetochores lose the metaphase alignment and tend to group around the CaM cores. In stages V and VI there is a striking dispersion of the CaM into the cytosol from its accumulation sites. At stages V and VI the kinetochores show a similar distribution to that in stage IV, and appear to maintain their structural integrity. Thus the striking dispersion of CaM is apparently correlated with the complete removal of residual microtubules in stages V and VI.

Effects on the pericentriolar matrix of drug-induced microtubule polymerisation

Taxoids, microtubule polymerising agents and suppressors of spindle microtubule dynamics, cause a characteristic and striking redistribution of CaM, involving rearrangement of components of the mitotic spindle with microtubules in complex multipolar patterns throughout the cytoplasm and accumulation of immunocytochemically detectable CaM in the centers of drug-induced asters, possibly analogous to normal spindle poles (De Brabander et al., 1981). Taxoids decrease the tubulin critical concentration, and could increase spontaneous microtubule nucleation in the cytoplasm. More recently, pulsed taxoid treatment of synchronised interphase HeLa cells was shown to cause disorganisation in centrosome replication and the asymmetric distribution of the non-centrosomal microtubule-focussing protein, NuMa (Paoletti et al., 1997). Dose-dependent mechanisms were proposed for the formation of: (1) monopolar spindles, where the centrioles and pericentriolar material do not redistribute; (2) bipolar spindles, with asymmetric distribution of the nuclear protein NuMa and pericentriolar material, which leads to a catastrophic exit from mitosis; and (3) multipolar asters, attributed to microtubule nucleation.

Our experimental protocol involves unsynchronised MDCK cells, treated continuously for 4 hours with a very low concentration of paclitaxel [~30-times lower than used previously (Paoletti et al., 1997)]. CaM is present at all the paclitaxel-induced multiple spindles, whether there is one pole (the case with no redistribution of the centrioles and pericentriolar matrix), or two, three, four or more poles. Fig. 6F-I and Movie 4 show the striking tendency of the CaM-containing structures present at the original spindle pole to divide. This strongly suggests that the effect of paclitaxel on cells that were possibly initially in prophase or metaphase is to induce the subdivision of the spindle pole/centrosome structure into CaM-containing multiple poles, which remain attached to the condensed chromosomal plate (Fig. 6B-D). We suggest that the multipolar structure could arise by paclitaxel-dependent suppression of spindle microtubule dynamics, with microtubule elongation provoking a relatively even split of the centrosomal matrix as indicated by the images in Fig. 6F-I and Movie 4. Since paclitaxel causes modified rigidity of microtubules, mechanical strain could also contribute to the splitting of the centrosomal matrix.

The intermediate steps in cells subjected to paclitaxel

treatment during late prophase and metaphase, after the separation of the two centrosomes, are presented schematically in Fig. 8. The CaM initially remains associated with kinetochore-to-pole microtubules as in control cells. However, at the spindle pole level, significant modifications take place. The CaM-EGFP appears to subdivide from its ring-like shape, along with entire fragments of the spindle, including microtubules and associated kinetochores and chromosomes. This takes place gradually to generate a multipolar spindle, with CaM in a ring-like structure at each of these poles. Certain 'scaffolding' proteins from the pericentriolar material may be involved (see below). Stable CaM-containing multipolar structures could then be produced by paclitaxel-dependent stabilisation of microtubules, followed by fragmenting of the spindle poles, which carry some CaM-containing pericentriolar material, and preserving the connectivity of microtubules in spindle-like shapes (Fig. 8).

Calmodulin-binding target proteins in the pericentriolar matrix

The spectroscopic characterisation of the purified fusion protein, CaM-EGFP, shows that it preserves the characteristics of the native calmodulin with respect to calcium, target peptide and protein binding. CaM-target interaction is critical for the diverse number of cellular functions performed by this protein, including the progression through the mitotic process (Rasmussen et al., 1992). Figs 7 and 8 illustrate that CaM localises in the mitotic spindle close to microtubules, its accumulation at certain sites of the spindle being dependent on the existence of some residual microtubule structures.

Ca^{2+} is known to be an important signal in cell division (Berridge et al., 1998), consistent with the idea that calmodulin acts in a Ca^{2+}-dependent fashion in initiating changes involved in the mitotic progression. However, in yeast (*S. cerevisae*), where calmodulin (yCaM) has been localised to the spindle pole-body (spb), yeast-expressing yCaM mutants with impaired calcium-binding function have been observed to show similar localisation with the calmodulin-binding protein, Spc110p (Geiser et al., 1991; Geiser et al., 1993). Spc110p is involved in the microtubule attachment to the core of the spb, which acts as a microtubule organising centre analogous to the centrosome in higher eukaryotes (Knop and Schiebel, 1997; Nguyen et al., 1998). This strongly supports our finding that CaM appears to be involved in the attachment of kinetochore microtubules to the centrosome. We have now expressed the EGFP fusion protein of mammalian 'null-calmodulin' mutated in all four Ca^{2+}-binding sequences (cf. Mukherjea et al., 1996) in both HeLa and MDCK cells (N.M., M.E. and P.M.B., unpublished). Throughout the cell cycle and in drug treatments the distribution of nullCaM-EGFP is similar to that of CaM-EGFP. This further suggests that the localisation of CaM in the mitotic spindle and at essential elements of the mitotic apparatus under disruptive conditions may be relatively insensitive to Ca^{2+} concentration.

Our experimental observations strongly suggest that CaM-containing pericentriolar material subdivides in a specific way, under the influence of microtubule perturbing drugs. The localisation of CaM at the pole requires both the presence of some intact polymerised microtubule structure, as well as certain spindle pole and centrosomal protein. These could determine the ring-like shape of CaM-EGFP at spindle poles in normal mitotic cells, and its presence at the paclitaxel-induced poles. CaM-EGFP from the core of the small star-like sub-structure appears to have the same centrosomal origin, but lacks this level of organisation.

γ-tubulin is a significant component of the pericentriolar matrix in control (Moudjou et al., 1996; Dictenberg et al., 1998) and taxol-treated metaphase cells, (Vorobjev et al., 2000), and is involved in centrosomal microtubule nucleation (Oakley and Oakley, 1989). However, antibody to γ-tubulin does not appear to label the star-like structure produced by depolymerising drugs (data not shown). This lack of colocalisation of calmodulin and centrosomal γ-tubulin is consistent with the co-existence of 'stars' with the remnants of the polar ring (Fig. 3A), since γ-tubulin remains localised in centrosomal structures in stage III of nocodazole perturbation (data not shown). It is also consistent with calmodulin localisation at spindle poles lacking centrioles in higher plant endosperm cells (Vantard et al., 1985). Thus calmodulin locates independently of γ-tubulin.

From the centrosomal proteins (for reviews, see Kalt and Schliwa, 1993; Andersen, 1999), several large pericentriolar coiled-coil proteins, suggested to function as scaffolds for microtubule-nucleating complexes and as binding sites for other proteins, have been identified as having CaM-binding motifs. Kendrin (PCNT2) and Spc110 share homology in this region (Flory et al., 2000) and they appear to bind the CaM in a Ca^{2+}-independent manner through a sequence that differs from the IQ motif. Alternatively, the abnormal *Drosophila* spindle protein (Asp) (Avides and Glover, 1999; Saunders et al., 1997), which has a similar scaffolding function, contains the Ca^{2+}-independent CaM-binding IQ-motif (Bahler and Rhoads, 2001), as does the recently identified centrosomal A-kinase anchoring protein (AKAP450) (Withczak et al., 1999; Gillingham and Munro, 2000). Although pericentrin, a component of the pericentriolar matrix (Doxsey et al., 1994), does not apparently possess a CaM-binding site, it is identified as an AKAP (Diviani et al., 2000), raising the possibility of a direct or indirect interaction with calmodulin. Evidence has been reported for indirect interaction of coiled-coil proteins with microtubules. Thus, kendrin recruitment to the centrosomal matrix may be partially microtubule dependent (Li et al., 2000); similarly cytoplasmic dynein transports pericentrin (together with γ-tubulin) onto centrosomes in a microtubule-dependent process (Young et al., 2000). The presence in the centrosomal matrix of coiled-coil proteins containing CaM-binding motifs could account for the CaM localisation reported in our work. Since the recruitment to the centrosomal structure of kendrin (and hence putatively CaM as well) is at least partially conditional on the integrity of the microtubule system, microtubule disassembly would be expected to impair the stability of the organelle, as we have observed.

Non-centrosomal proteins, such as cytoplasmic dynein, dynactin, NuMA and Eg5, and a minus-end-directed kinesin-related protein, appear to be required for the microtubule focusing and organisation of free microtubule minus ends (Gaglio et al., 1997). Although these proteins do not apparently themselves bind CaM directly, they may contribute to the microtubule-dependent stability of the centrosome and the

maintenance of the ring-like shape (seen as the typical locus of centrosomal CaM) at normal and paclitaxel-induced poles.

Our results show an apparent localisation of CaM with kinetochores at an advanced, but still incomplete, stage of microtubule disassembly, but so far none of the kinetochore stable or transient proteins (Saffery et al., 2000) has been identified as a CaM-binding protein. Microtubule-associated proteins (MAPs) and motor proteins are potential targets for calmodulin, more likely by indirect rather than direct mechanisms. Dynein and kinesin are used in the assembly of the mitotic spindle and for the microtubule sliding movement during the progression of mitosis (Wittmann et al., 2001; Sharp et al., 2000). Motors may also be involved in the function of the kinetochore, where dynein is found (Pfarr et al., 1990; Steuer et al., 1990). Another motor protein proven to localise in regions rich in microtubules, and in interphase and in mitotic cells, is myosin V, which plays a role in the efficiency of the cell division in culture (Espreafico et al., 1998; Wu et al., 1998). Myosin V localises in a ring-like polar structure similar to the calmodulin distribution (Erent et al., 1999), and it becomes dispersed by nocodazole treatment (Tsakraklides et al., 1999). It has been proposed that myosin Va interacts with microtubules by associating with dynein through shared 8 kDa light chains (Wu et al., 2000). Like many unconventional myosins, myosin V possesses multiple IQ motifs for Ca^{2+}-independent CaM binding. Moreover, the presence of myosin V close to calmodulin in the spindle and spindle pole, and the distribution of the null-mutant of CaM at the same sites (N.M., M.E. and P.M.B., unpublished) suggest that myosin V is another candidate target protein for Ca^{2+}-independent binding of calmodulin in the mitotic spindle. The relationship between calmodulin, myosin V and pericentriolar proteins is therefore highly relevant to the structure and dynamic function of the centrosomal matrix.

In conclusion, microtubule destabilising and stabilising treatments both produce a selective subdivision of the centrosomal matrix, with the release of distinct substructures containing CaM-binding proteins. Microtubule depolymerisation (by nocodazole or vinblastine) produces the small star-like structures, which may represent an anchoring mechanism for kinetochore microtubules. By contrast, microtubule stabilisation (by taxoids) causes limited subdivision of the pericentriolar material, in a relatively orderly way, to produce the multiple CaM-containing ring-like poles. These results further suggest that the integrity of the centrosomal matrix as a complex dynamic structure depends upon interactions with normal spindle-pole microtubules. Key questions arising from this work are: (1) the identity of potential calmodulin targets in the pericentriolar matrix; (2) their possible association with microtubules in this matrix; and (3) the continued association of these calmodulin-binding proteins with calmodulin, once microtubules are fully disassembled. Among potential candidates as targets, known to bind calmodulin in either Ca^{2+}-dependent or Ca^{2+}-independent processes, are the scaffolding coiled-coil proteins, kendrin (PCNT2) and AKAP450, and myosin V, a chemo-mechanical motor protein. Calmodulin could therefore have a significant role in regulating the function of such targets in establishing and maintaining structure and function in the pericentriolar matrix in relationship to the dynamic nature of the microtubule cytoskeleton.

We acknowledge the generous gift of CREST serum from Guy Keryer and J. C. Courvallin (Institut Curie, Paris); calmodulin antibody from David Sacks (Harvard University); the Camkinase-I 1-321 construct from Angus Nairn (Rockefeller University, NY); and the modified pET vector from G. Stier (EMBL, Heidelberg). We thank Richard McIntosh (University of Colorado, Denver), Guy Keryer (Institut Curie, Paris), Kate Beckingham (Rice University, Huston) and Derek Stemple (NIMR, London) for advice and useful discussions. We appreciate substantial assistance from Kate Sullivan and Stamatis Pagakis of the Confocal and Image Analysis Laboratory, and Jo Brock and Frank Johnson of Photographics Services Section, NIMR. N.M. acknowledges the support of a NATO-Royal Society Postdoctoral Fellowship (99B/NATO) for part of this work.

References

Andersen, S. S. (1999). Molecular characteristics of the centrosome. *Int. Rev. Cytol.* **187**, 51-109

Avides, M. C. and Glover, D. M. (1999). Abnormal spindle protein Asp, and the integrity of mitotic centrosomal microtubule organising centers. *Science* **283**, 1733-1735.

Bahler, M. and Rhoads, A. (2002). Calmodulin signaling via the IQ motif. *FEBS Lett.* **513**, 107-113.

Berridge, M. J., Bootman, M. D. and Lipp, P. (1998). Calcium a life and death signal. *Nature* **395**, 645-648.

Browne, J. B., Strom, M., Martin, S. R. and Bayley, P. M. (1997). The role of β-sheet interactions in domain stability, folding, and target recognition reactions of calmodulin. *Biochemistry* **36**, 9550-9561.

Chin, D. and Means, A. R. (2000). Calmodulin: a prototypical calcium sensor. *Trends Cell Biol.* **10**, 322-328.

De Brabander, M., Geuens, G., Nuydens, R., Willebrords, R. and de Mey, J. (1981). Taxol induces the assembly of free microtubules in living cells and blocks the organising capacity of the centrosomes and kinetochores. *Proc. Natl. Acad. Sci. USA* **78**, 5608-5612.

De Mey, J., Moeremans, M., Geuens, G., Nuydens, R., van Belle, H. and de Brabander, M. (1980). Immunocytochemical evidence for the association of calmodulin with microtubules of the mitotic apparatus. In *Microtubules and Microtubules Inhibitors* (ed. M. De Brabander and J. De Mey), pp. 227-241. North Holland: Elsevier.

Dictenberg, J. B., Zimmerman, W., Sparks, C. A., Young, A., Vidair, C., Zheng, Y., Carrington, W., Fay, F. S. and Doxey, S. J. (1998). Pericentrin and γ-tubulin form a protein complex and are organised into a novel lattice at centrosome. *J. Cell Biol.* **141**, 163-174.

Diviani, D., Lagenberg, L. K., Doxey, S. J. and Scott, J. D. (2000). Pericentrin anchors protein kinase A at the centrosome through a newly identified RII-binding domain. *Curr. Biol.* **10**, 417-420.

Doxsey, S. J., Stein, P., Evans, L., Calarco, P. D. and Kirschner, M. (1994). Pericentrin, a highly conserved centrosome protein involved in microtubule organisation. *Cell* **76**, 639-650.

Erent, M., Browne, J. P., Pagakis, S. and Bayley, P. M. (1999). Association of calmodulin with cytoskeletal structures at different stages of HeLa cell division, visualised by a calmodulin-EGFP fusion protein. *Molec. Cell. Biol. Res. Commun.* **1**, 209-215.

Espreafico, E. M., Coling, D. E., Tsakralides, V., Krogh, K., Wolenski, J. S. and Kachar, B. (1998). Localisation of myosin V in the centrosome. *Proc. Natl. Acad. Sci. USA.* **95**, 8636-8641.

Findlay, W. A., Martin, S. R. Beckingham, K. and Bayley, P. M. (1995). Recovery of native structure by calcium binding site mutants of calmodulin upon binding of sk-MLCK target peptides. *Biochemistry* **34**, 2087-2094.

Flory, M. R., Moser, M. J., Monnat, R. J. and Davis, T. N. (2000). Identification of human centrosomal calmodulin binding protein that shares homology with pericentrin. *Proc. Natl. Acad. Sci USA.* **97**, 5919-5923.

Gaglio, T., Dionne, M. A. and Compton, D. A. (1997). Mitotic spindle poles are organised by structural and motor protein in addition to centrosome. *J. Cell Biol.* **138**, 1055-1066.

Geiser, J. R, van Tuinen, D., Brockerhoff, S. E., Neff, M. M. and Davis, T. N. (1991). Can calmodulin function without calcium? *Cell* **65**, 949-959.

Geiser, J. R., Sundberg, H. A., Chang, B. H., Muller, E. G. and Davis, T. N. (1993). The essential mitotic target of calmodulin is the 110-kilodalton component of the spindle pole body in *Saccharomyces cerevisiae*. *Mol. Cell. Biol.* **13**, 7913-7924.

Gillingham, A. K. and Munro, S. (2000). The PACT domain, a conserved

centrosomal targeting motif in the coiled-coil proteins AKAP450 and pericentrin. *EMBO Rep.* **6**, 524-529.

Gregorio, C. C., Trombitas, K., Centner, T., Kolmerer, B., Stier, G., Kunke, K., Suzuki, K., Obermayr, F., Herrmann, B., Granzier, H. et al. (1998). The NH2 terminus of titin spans the Z-disc: its interaction with a novel 19-kD ligand (T-cap) is required for sarcomeric integrity. *J Cell Biol.* **143**, 1013-1027.

Jordan, M. A. and Wilson, L. (1998). Use of drugs to study role of microtubule assembly dynamics in living cells. *Methods Enzymol.* **298**, 252-276.

Jordan, M. A. and Wilson, L. (1999). The use and action of drugs in analysing mitosis. *Methods Cell Biol.* **61**, 267-295.

Jordan, M. A., Thrower, D. and Wilson, L. (1992). Effects of vinblastine, podophyllotoxin and nocodazole on mitotic spindles. Implications for the role of microtubule dynamics in mitosis. *J. Cell Sci.* **102**, 401-416.

Kalt, A. and Schliwa, M. (1993). Molecular components of the centrosome. *Trends Cell Biol.* **3**, 118-128.

Kneen, M., Farinas, J., Yuxin, L. and Verkman, A. S. (1998). Green Fluorescent Protein as a noninvasive intracellular pH indicator. *Biophys. J.* **74**, 1591-1599.

Knop, M. and Schiebel, E. (1997). Spc98p and Spc97p of the yeast γ-tubulin complex mediate binding to the spindle pole body via their interaction with Spc110p. *EMBO J.* **16**, 6985-6995.

Li, C., Heim, R., Lu, P., Pu, Y., Tsien, R. Y. and Chang, D. C. (1999). Dynamic redistribution of calmodulin in HeLa cells during cell division as revealed by a GFP-calmodulin fusion technique. *J. Cell Sci.* **112**, 1567-1577.

Li, Q., Hansen, D., Kililea, A., Joshi, H. C., Palazzo, R. E. and Balczon, R. (2000). Kendrin/pericentrin-B, a centrosome protein with homology to pericentrin that complexes with PCM-1. *J. Cell Sci.* **114**, 797-809.

Linse, S., Brodin, P., Johansson, C., Thulin, E., Grundstrom, T. and Forsen, S. (1988). The role of surface charges in ion binding. *Nature* **335**, 651-652.

Linse, S., Helmersson, A. and Forsen, S. (1991). Calcium binding to calmodulin and its globular domains. *J. Biol. Chem.* **266**, 8050-8054.

Llopis, J., McCaffery, J. M., Miyawaki, A., Farquar, M. G. and Tsien, R. Y. (1998). Measurement of cytosolic, mitochondrial and Golgi pH in single living cells with green fluorescent proteins. *Proc. Natl. Acad. Sci. USA* **95**, 6803-6808.

Martin, S. R., Schilstra, M. J. and Bayley, P. M. (1993). Dynamic instability of microtubules: Monte Carlo simulation and application to different types of microtubule lattice. *Biophys. J.* **65**, 578-596.

Martin, S. R., Bayley, P. M, Brown, S. E., Porumb. T., Zhang, M. and Ikura, M. (1996). Spectroscopic characterisation of a high affinity calmodulin-target peptide hybrid molecule. *Biochemistry* **35**, 3508-3517.

Mitsuyama, F. and Kanno, T. (1993). Localisation of Ca^{2+} calmodulin to the kinetochore of C6 glioma: an investigation of the anti-tumour effects of calmodulin antagonists in the treatment of brain tumours. *Neurol. Res.* **15**, 131-135.

Moudjou, M., Bordes, N., Paintrand, M. and Bornens, M. (1996). gamma-Tubulin in mammalian cells: the centrosomal and the cytosolic forms. *J Cell Sci.* **109**, 875-887.

Mukherjea, P., Maune, J. F. and Beckingham, K. (1996). Interlobe communication in multiple calcium-binding site mutants of *Drosophila* calmodulin. *Protein Sci.* **5**, 468-477.

Ngan, V. K., Bellman, K., Hill, B. T., Wilson, L. and Jordan, M. A. (2001). Mechanism of mitotic block and inhibition of cell proliferation by the semisynthetic vinca alkaloids vinorelbine and its newer derivative vinflunine. *Mol. Pharmacol.* **60**, 225-232.

Nguyen, T., Vinh, D. B. N., Crawford, D. K. and Davis, T. N. (1998). A genetic analysis of interactions with Spc110p reveals distinct functions of Spc97p and Spc98p, components of the yeast γ-tubulin complex. *Mol. Biol. Cell* **9**, 2201-2216.

Oakley, C. E. and Oakley, B. R. (1989). Identification of γ-tubulin, a new member of the tuublin superfamily encoded by MipA gene of *Aspergillus nidulans*. *Nature* **338**, 662-664.

Paoletti, A., Giocanti, N., Favaudon, V. and Bornens, M. (1997). Pulse treatment of interphase HeLa cells with nanomolar doses of docetaxel affects centrosome organisation and leads to catastrophic exit of mitosis. *J. Cell Sci.* **110**, 2403-2415.

Pfarr, C. M., Coue, M., Grissom, P. M., Hays, T. S., Porter, M. E. and McIntosh, J. R. (1990). Cytoplasmic dynein is localised to kinetochores during mitosis. *Nature* **345**, 263-265.

Rasmussen, C. D., Lu, K. P., Means, R. L. and Means, A. R. (1992). Calmodulin and cell cycle control. *J. Physiol.* **86**, 83-88.

Rhoads, A. R. and Friedberg, F. (1997). Sequence motifs for calmodulin recognition. *FASEB J.* **11**, 331-340.

Sacks, D. B., Porter, S. E., Landenson, J. H. and McDonald, J. M. (1991). Monoclonal antibody to calmodulin: development characterisation and comparison with polyclonal anti-calmodulin antibodies. *Anal. Biochem.* **194**, 369-377.

Saffery, R., Irvine, D. V., Griffits, B., Kalitsis, P., Wordeman, L. and Choo, K. H. (2000). Human centromeres and neocentromeres show identical distribution patterns of >20 functionally important kinetochore-associated proteins. *Hum. Molec. Genet.* **9**, 175-185.

Saunders, R. D., Avides, M. C., Howard, T., Gonzales, C. and Glover, D. M. (1997). The *Drosophila* gene abnormal spindle encodes a novel microtubule associated protein that associates with the polar regions of the mitotic spindle. *J. Cell Biol.* **137**, 881-890.

Sellitto, C. and Kuriyama, R. (1988). Distribution of pericentriolar material in multiple spindles induced by colcemid treatment in Chinese hamster ovary cells. *J. Cell Sci.* **89**, 57-65.

Sharp, D. J., Rogers, G. C. and Scholey, J. M. (2000). Microtubule motors in mitosis. *Nature* **407**, 41-47.

Stemple, D. L., Sweet, S. C., Welsh, M. J. and McIntosh, J. R. (1988). Dynamics of a fluorescent calmodulin analog in the mammalian mitotic spindle at metaphase. *Cell Motil. Cytoskeleton* **9**, 231-242.

Steuer, E. K., Wordeman, L., Schroeder, T. A. and Shetz, M. P. (1990). Localisation of cytoplasmic dynein to mitotic spindles and kinetochore. *Nature* **345**, 266-268.

Sweet, S. C., Rogers, C. M. and Welsh, M. J. (1988). Calmodulin stabilisation of kinetochore microtubule structure to the effect of nocodazole. *J. Cell Biol.* **107**, 2243-2251.

Tsakraklides, V., Krogh, K., Wang, L., Bizario, J. C. S., Larson, R. E., Espreafico, E. M. and Wolensk, J. S. (1999). Subcellular localisation of GFP-myosin-V in live mouse melanocytes. *J. Cell Sci.* **112**, 2835-2865.

Vantard, M., Lambert, A. M., de Mey, J., Piquot, P. and van Eldik, L. J. (1985). Characterisation and immunocytochemical distribution of calmodulin in higher plant endosperm cells: localisation in the mitotic apparatus. *J. Cell Biol.* **101**, 488-499.

Vorobjev, I. A., Uzbekov, R. E., Komarova, Y. A. and Alieva, I. B. (2000). γ-Tubulin distribution in interphase and mitotic cells upon stabilisation and depolymerization of microtubules. *Membr. Cell Biol.* **14**, 219-235.

Wadsworth, P. and McGrail, M. (1990). Interphase microtubule dynamics are cell type specific. *J. Cell Sci.* **95**, 23-32.

Welsh, M. J., Dedman, J. R., Brinkley, B. R. and Means, A. R. (1979). Tubulin and calmodulin. Effects of microtubule and microfilament inhibitors on localisation in the mitotic apparatus. *J. Cell Biol.* **81**, 624-634.

Willingham, M. C., Wehland, J., Klee, C. B., Richert, N. D., Rutherford, A. V. and Pastan, I. H. (1983). Ultrastructural immunocytochemical localization of calmodulin in cultured cells. *J. Hystochem. Cytochem.* **4**, 445-461.

Withczak, O., Skalhegg, B. S., Keryer, G., Bornens, M., Tasken, K., Jahnsen, T. and Orstavik, S. (1999). Cloning and characterisation of a cDNA encoding an A-kinase anchoring protein located in the centrosome, AKAP 450. *EMBO J.* **18**, 1858-1999.

Wittmann, T., Hyman, A. and Desai, A. (2001). The spindle: a dynamic assembly of microtubules and motors. *Nat. Cell Biol.* **3**, E28-E34.

Wu, X., Kocher, B., Qin, W. and Hammer, J. A. (1998). Myosin Va associates with microtubule-rich domains in both interphase and dividing cells. *Cell Motil. Cytoskeleton* **40**, 286-303.

Wu, X., Goeh, J. and Hammer, J. A. (2000). Functions of unconventional myosins. *Curr. Opin. Cell Biol.* **12**, 42-51.

Yokokura, H., Picciotto, M. R., Nairn, A. C. and Hidaka, H. (1995). The regulatory region of calcium/calmodulin-dependent protein kinase I contains closely associated autoinhibitory and calmodulin-binding domains. *J. Biol. Chem.* **270**, 23851-23859.

Young, A., Dictenberg. J. B., Purohit, A., Tuft, R. and Doxsey, S. J. (2000). Cytoplasmic dynein-mediated assembly of pericentrin and tubulin onto centrosomes. *Mol. Biol. Cell* **11**, 2047-2056.

Zavortink, M., Welsh, M. J. and McIntosh, J. R. (1983). The distribution of CaM in living mitotic cells. *Exp. Cell Res.* **149**, 375-385.